P-ISSN: 2798-1134 | E-ISSN: 2797-3549 | DOI: 10.52562/injoes.2025.1767

Indonesian Journal of Earth Sciences

http://journal.moripublishing.com/index.php/injoes

| Research Article |

Analysis of the Relationship Between Resistivity and Seawater Moisture Content Percentage in Loose Sand Medium on the Yogyakarta Coastal Area

Yudha Agung Pratama[1]*, Mycelia Paradise[2], Suharsono[1], Wahyu Hidayat[1], Ajimas Pascaning Setiahadiwibowo[1]

[1]Department of Geophysical Engineering, UPN "Veteran" Yogyakarta, Yogyakarta 55283, Indonesia
[2]Department of Mining Engineering, Institut Teknologi Nasional Yogyakarta, Yogyakarta 55281, Indonesia
**Correspondence: yudha.agung@upnyk.ac.id*

Received: 02 August 2025 / Accepted: 05 September 2025 / Published: 08 September 2025

Abstract: This study investigates the effect of seawater moisture content on the resistivity of unconsolidated sand in the coastal region of Yogyakarta. Laboratory experiments were conducted using a standard ASTM G-57 soil box with samples prepared at varying percentages of seawater moisture content. The results indicate that increasing seawater content in the sediment medium leads to an exponential decrease in resistivity. A mathematical relationship was established in the form of a power function: $R=1145.7MC^{-2.23}$. Resistivity values tend to stabilize when the moisture content exceeds 13%. A resistivity range of 0.8–2.8 Ω·m is proposed as a cut-off for identifying seawater intrusion in coastal areas. These findings provide an important contribution to the development of geoelectrical methods for monitoring seawater intrusion and evaluating groundwater quality in coastal regions, which can serve as a basis for sustainable water resource management.

Keywords: Resistivity; moisture content; seawater

INTRODUCTION

Residential development in coastal areas has undergone significant change. Between 1996 and 2003, the extent of settlements increased by 0.24% per year, with the area of residential housing alone expanding by 6.14%. Much of this growth occurred near tourism facilities (Suritohardoyo, 2016). Spatial planning plays a crucial role in ensuring sustainable land use in Bantul, particularly in the implementation of zoning regulations (Nugroho et al., 2023). In Gunungkidul, approximately 96,983 ha (81.2%) of land is designated as tourism areas, while 24,460 ha (18.8%) is categorized as conditionally suitable in accordance with Government Regulation No. 50 of 2011, which regulates public infrastructure and tourism facilities, including the provision of freshwater resources (Afriyanto et al., 2020). However, uncoordinated development in coastal regions poses environmental risks, potentially impacting local communities and urban infrastructure (Laiskodat & Lay, 2023). These conditions highlight the need for continuous subsurface monitoring, particularly of groundwater dynamics and seawater intrusion driven by coastal development. Within this context, geoelectrical methods are widely applied because they exploit the electrical properties of geological media to reveal subsurface characteristics, particularly resistivity variations. Numerous studies have utilized resistivity measurements for detecting seawater intrusion.

Across various coastal regions in Indonesia, seawater intrusion is consistently characterized by low resistivity values, particularly in sandy, gravelly, and other porous lithologies that are easily saturated with seawater. However, the resistivity thresholds identified for seawater intrusion differ widely among studies. For example, in Laimeo-Ulu Sawa, Sawa District, seawater intrusion was inferred in sand and gravel layers with resistivity values ranging between 0.5–5 Ω·m (Arliska et al., 2022). In Kampung Baru Village, seawater intrusion zones were identified with resistivity values between 0.40–6.40 Ω·m (Astutik et al., 2016). A narrower range was reported in Samudra Bungus, where seawater intrusion was indicated by values of 0.79–3.84 Ω·m (Putri et al., 2020). In Mempawah, seawater intrusion in sandy lithology was interpreted within a range of 0.262–7.36 Ω·m (Muslim et al., 2021). From these studies, resistivity values associated with seawater intrusion were generally observed between 0.262–7.36 Ω·m, with the lowest values below 1 Ω·m.

Other studies have reported higher ranges. At Gandoriah Beach, seawater intrusion in sandy and gravelly layers was associated with resistivity values of 2.25–4.96 Ω·m (Mela, 2023). In Malangke, seawater intrusion was inferred within a range of 1.7–5.9 Ω·m (Jusmi & Bakri, 2020), generally above 1.7 Ω·m but within a narrower interval. At Candidasa, seawater intrusion was interpreted in areas with resistivity values of 0.5–30 Ω·m (Pujianiki & Simpen, 2018). In Kaligawe, seawater intrusion was identified within 2.07–13.2 Ω·m (Hastuti et al., 2015). On Karimunjawa Island, intrusion led to the conversion of freshwater into brackish water, with resistivity values ranging from 4.95–31.9 Ω·m (Pryambodo & Prihantono, 2017). In another study in Mempawah, seawater intrusion was identified with values ranging from 0.15–28.10 Ω·m (Muhardi et al., 2020). These findings illustrate that seawater intrusion can be associated with resistivity values extending into tens of Ω·m, with a general interpretive range of 0.5–31.9 Ω·m.

The wide variation in resistivity ranges reported across different regions—from below 1 Ω·m to several tens of Ω·m—indicates that while low resistivity is a reliable indicator of seawater intrusion, the threshold values are strongly site-dependent. This underscores the importance of conducting experimental studies to establish reference values that are more appropriate for local geological conditions. An experimental approach allows for the determination of a quantitative relationship between moisture content (seawater) in a material and its resistivity, thereby providing a more reliable basis for field geoelectrical interpretation. Such localized studies are essential to establish resistivity thresholds aligned with specific geological settings, enabling clearer, more measurable, and applicable delineation of seawater intrusion in support of sustainable groundwater resource management.

METHOD

Study Location and Sampling

This study was conducted in both laboratory and field settings. Laboratory analyses were carried out at the Geophysics Laboratory of UPN "Veteran" Yogyakarta, where sample processing and data interpretation were performed. Sand samples were collected from three coastal sites representing different geological settings: (i) Gunungkidul, dominated by karst formations; (ii) Parangtritis, characterized by volcanic deposits and active beach sands; and (iii) Kulonprogo, representing older sedimentary formations. The samples consisted of surface loose sand. The selection of these sites aimed to obtain a diverse dataset that reflects varying geological characteristics, allowing for comparative analysis. The sampling locations are shown in Figure 1.

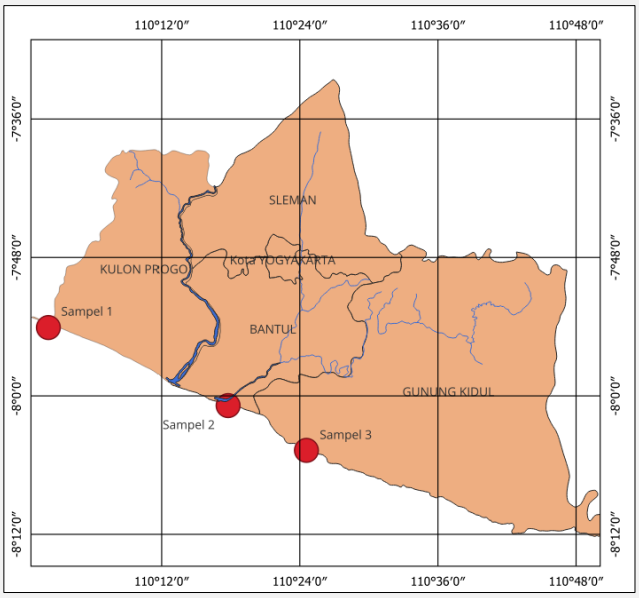

Figure 1. Study area (sampling locations indicated by red points).

Sample preparation involved reducing the natural water content of the loose sand samples in accordance with ASTM D2216. Seawater used in the experiments was collected from a single source to

maintain consistency. The preparation procedure followed ASTM G57-06, with seawater added to the sand to represent different levels of moisture content. For each test, 150 g of loose sand was weighed, and seawater was added in increments of 5 ml for each resistivity measurement. The ratio between the sand mass and seawater volume was used to calculate the moisture content. Each mixture was homogenized in a closed container before being placed into the soil box for testing.

Soil Box Configuration

Resistivity measurements were performed using an experimental resistivity method with a soil box designed for unconsolidated materials, following ASTM G57-06 standards with a four-electrode Wenner configuration. The soil box had a volume of 80 ml (80 cm³). Its cross-sectional area (A), when filled, divided by the electrode spacing (L) produced an A/L ratio of 1 cm. The detailed dimensions of the soil box were as follows: cross-sectional area 3.0 cm × 2.4 cm = 7.2 cm², electrode spacing 7.2 cm, giving A/L = 1 cm.

Measurement Procedure

Current injection was performed using a variable power supply generating a sinusoidal waveform at 97 Hz with a maximum voltage of 12 V. Signal stability and data quality were monitored with a GDS-1102 oscilloscope. Current was measured using a Fluke 116 multimeter with a resolution of 0.1 μA and accuracy of (1.5% + 3 digits), while voltage was measured using a Sanwa CD800a multimeter with a resolution of 0.1 mV and accuracy of (0.7% + 3 digits). All measurements were processed and analyzed to obtain resistivity values.

Uncertainty Analysis

Uncertainty analysis was performed for voltage (V) and current (I) measurements, each with its respective instrument accuracy. The combined uncertainty for a function $Q = f(x_1, x_2, \ldots, x_n)$ is expressed as:

$$\Delta Q = \sqrt{\left(\frac{\partial f}{\partial x_1} \cdot \Delta x_1\right)^2 + \left(\frac{\partial f}{\partial x_2} \cdot \Delta x_2\right)^2 + \ldots} \quad (1)$$

In this study, Q = f(V, I), and resistance (R) was derived from Ohm's Law:

$$R = \frac{V}{I} \quad (2)$$

Partial derivatives yield:

$$\frac{\partial R}{\partial V} = \frac{1}{I}, \qquad \frac{\partial R}{\partial I} = -\frac{V}{I^2} \quad (3)$$

$$\Delta Q = \sqrt{\left(\frac{\partial f}{\partial V} \cdot \Delta V\right)^2 + \left(\frac{\partial f}{\partial I} \cdot \Delta I\right)^2} \quad (4)$$

Thus, the combined uncertainty in R is:

$$\Delta R = \sqrt{\left(\frac{1}{I}\Delta V\right)^2 + \left(-\frac{1}{I^2}\Delta I\right)^2} \quad (5)$$

$$\Delta R = R \cdot \sqrt{\left(\frac{\Delta V}{V}\right)^2 + \left(\frac{\Delta I}{I}\right)^2} \quad (6)$$

$$\frac{\Delta R}{R} = \sqrt{\left(\frac{\Delta V}{V}\right)^2 + \left(\frac{\Delta I}{I}\right)^2} \quad (7)$$

With V representing voltage and I representing current in Equation (2), the resistance R is derived from two measured quantities, as shown in Equation (3). Consequently, the uncertainty in R is influenced by the relative uncertainties of both variables. The symbols ΔV and ΔI denote the absolute uncertainties in the voltage and current measurements, respectively, while $\Delta V/V$ and $\Delta I/I$ represent their relative uncertainties. By applying the root-sum-square method of error propagation, these relative uncertainties are combined to provide an estimate of the total relative uncertainty in resistance. Equation (7) expresses the form of the combined uncertainty used in this study. The values of ΔV and ΔI were determined based on the accuracy ranges specified for each instrument.

Data Acquisition

A total of 108 measurements were conducted. For each of the three sampling sites, eight levels of seawater moisture content were tested. Each condition was measured three times using different injection currents, resulting in 72 measurements with seawater. An additional 36 measurements were conducted on dry samples (0% seawater content). Together, these datasets formed the basis of the resistivity analysis.

RESULTS & DISCUSSION

The results of this study are presented based on experimental measurements and subsequent analysis. Data are displayed in both graphical and descriptive form. Figure 2 shows the overall distribution of the measured samples. A clear distinction is observed between dry samples and those treated with seawater. Dry samples exhibit high resistivity values, ranging from approximately 1,944.6 to 2,180.6 Ω·m, with relatively narrow variability. In contrast, seawater-treated samples display much lower resistivity values, ranging from 0.8 to 99.3 Ω·m, with greater variation among replicates. This pattern indicates that treatments such as seawater addition substantially increase the electrical conductivity of the material. The presence of fluid within pore spaces lowers resistivity, as dissolved ions enhance the ability of the medium to conduct electrical current. The marked differences highlight that moisture content is a dominant factor influencing resistivity.

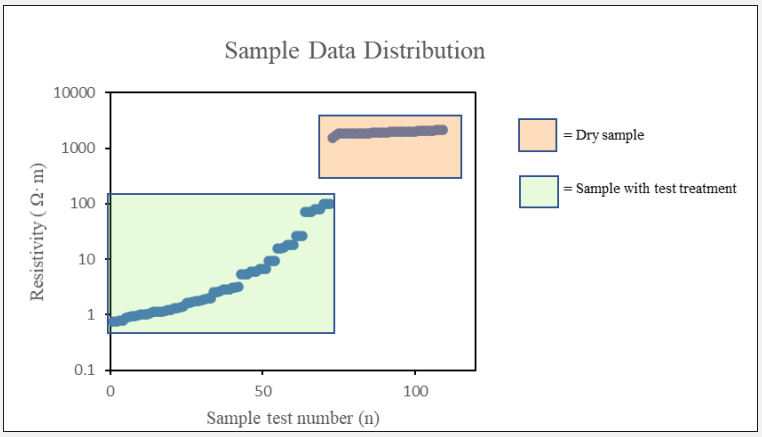

Figure 2. Total dataset from the resistivity experiments and the distribution of treated and untreated samples.

The overall range of resistivity for samples with seawater moisture content was 0.8–99.3 Ω·m. Compared with earlier studies, this range is broader and extends to relatively higher resistivity values. For instance, seawater intrusion was reported with resistivity values of 0.5–30 Ω·m at Candidasa (Pujianiki & Simpen, 2018), 4.95–31.9 Ω·m on Karimunjawa Island (Pryambodo & Prihantono, 2017), and 0.15–28.10 Ω·m in Mempawah (Muhardi et al., 2020). In this study, a moisture content of 3.3% was not yet fully representative of saturated conditions, as seawater only partially filled pore spaces. Consequently, resistivity values obtained under this condition remained higher than those expected under full saturation.

Figure 3 illustrates the experimental results for samples collected from Kulonprogo. Resistivity decreased systematically with increasing seawater content, ranging from 0.8 to 99.0 Ω·m. The relationship between seawater content (x) and resistivity (y) followed a power law, expressed as:

$$y = 1516.2x^{-2.343} \quad (8)$$

In this equation, the constant 1516.2 serves as a scaling factor, while the negative exponent (−2.343) indicates the rapid decline in resistivity as seawater content increases. At low concentrations (1–3%), resistivity remained relatively high but decreased sharply with additional seawater. At higher concentrations (above 20%), resistivity values approached a minimum and became less sensitive to further increases in seawater content. This nonlinear pattern demonstrates a steep initial decline followed by a gradual stabilization at higher concentrations.

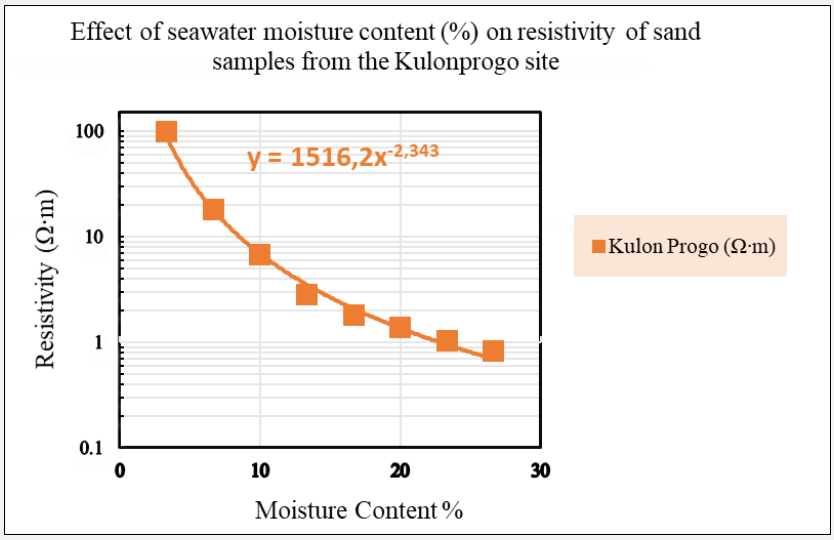

Figure 3. Effect of seawater moisture content (%) on resistivity for Kulonprogo sand samples.

Table 1. Relationship between seawater content and resistivity of unconsolidated sand samples from Congot Beach, Kulonprogo

No	Seawater MC (%)	Resistivity (Ω·m)	Accuracy Range (Ω·m)
1	0	2062.6 ± 118.0	1944.6 – 2180.6
2	3.3	99.3 ± 1.82	97.5 – 101.1
3	6.7	18.2 ± 0.34	17.9 – 18.5
4	10	6.7 ± 0.13	6.5 – 6.8
5	13.3	2.8 ± 0.06	2.8 – 2.9
6	16.7	1.8 ± 0.04	1.7 – 1.8
7	20	1.4 ± 0.04	1.3 – 1.4
8	23.3	1.0 ± 0.03	1.0 – 1.1
9	26.7	0.8 ± 0.03	0.8 – 0.8

Dry samples (0%) exhibited very high resistivity values (2,062.6 Ω·m), reflecting the insulating nature of sand in the absence of conductive pore fluids. The addition of seawater led to a significant reduction in resistivity. At 3.3% moisture content, resistivity had already dropped to 99.3 Ω·m, indicating the influence of free ions (Na^+, Cl^-) from seawater in enhancing conductivity. At 6.7% seawater content, resistivity fell further to 18.2 Ω·m, and at 10% to 6.7 Ω·m. At the highest concentration tested (26.7%), resistivity stabilized at a minimum of 0.8 Ω·m. This pattern confirms the strong inverse relationship between seawater content and resistivity: the higher the seawater saturation, the lower the resistivity.

Figure 4 presents results from Bantul samples. The same declining trend is evident, with resistivity values ranging from 0.8 to 71.4 Ω·m. The relationship is described by a power law function:

$$y = 979.12x^{-2.226} \quad (9)$$

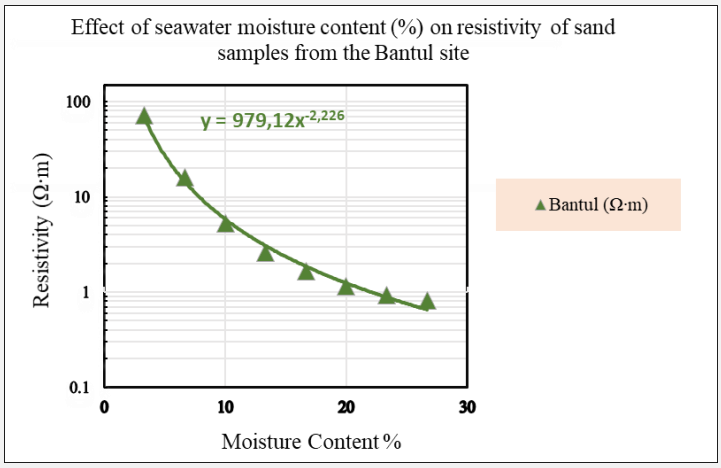

Figure 4. Effect of seawater moisture content (%) on resistivity for Bantul sand samples.

Table 2. Relationship between seawater content and resistivity of unconsolidated sand samples from Depok Beach, Bantul

No	Seawater MC (%)	Resistivity (Ω·m)	Accuracy Range (Ω·m)
1	0	1970.4 ± 83.07	1887.3 – 2053.4
2	3.3	71.4 ± 1.31	70.0 – 72.7
3	6.7	15.9 ± 0.30	15.6 – 16.2
4	10	5.3 ± 0.10	5.1 – 5.3
5	13.3	2.6 ± 0.06	2.6 – 2.6
6	16.7	1.7 ± 0.04	1.6 – 1.7
7	20	1.2 ± 0.03	1.1 – 1.2
8	23.3	0.9 ± 0.03	0.9 – 1.0
9	26.7	0.8 ± 0.03	0.8 – 0.8

For Bantul sands, the resistivity of dry samples (0% seawater) was 1,970.4 Ω·m, again reflecting insulating conditions. At 3.3% seawater content, resistivity dropped sharply to 71.4 Ω·m, while at 6.7% it was reduced to 15.9 Ω·m. With seawater levels above 13.3%, resistivity values stabilized, ranging between 2.6 Ω·m and 0.8 Ω·m at maximum saturation. This indicates that at high salinity, resistivity approaches a minimum threshold, with additional seawater exerting only a marginal effect on conductivity.

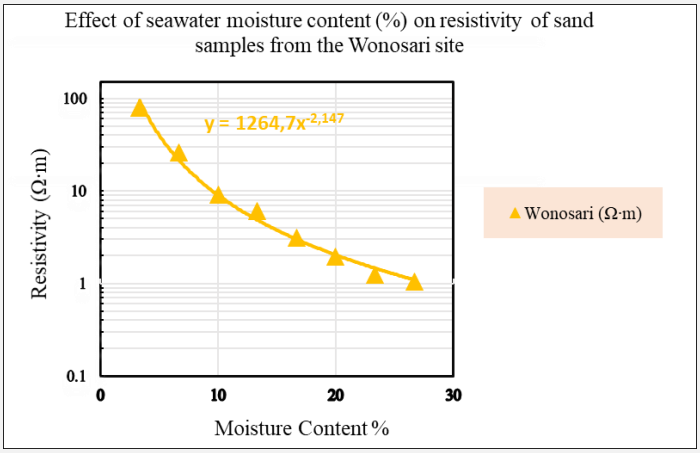

Figure 5. Effect of seawater moisture content (%) on resistivity of sand samples from Wonosari.

Figure 5 presents the experimental results for sand samples collected from Wonosari. Similar to the other sites, resistivity decreased systematically with increasing seawater content, ranging from 0.8 to 78.6 Ω·m. The relationship between seawater content (x) and resistivity (y) was modeled by a power law:

$$y = 1264.7x^{-2.147} \quad (10)$$

Table 3. Relationship between seawater content and resistivity of unconsolidated sand samples from Ngunggah Beach, Gunungkidul (Wonosari)

No	Seawater MC (%)	Resistivity (Ω·m)	Accuracy Range (Ω·m)
1	0	1867.4 ± 101.38	1766.0 – 1968.7
2	3.3	78.6 ± 1.44	77.2 – 80.0
3	6.7	25.9 ± 0.48	25.4 – 26.4
4	10	9.2 ± 0.17	9.0 – 9.3
5	13.3	6.0 ± 0.12	5.9 – 6.1
6	16.7	3.1 ± 0.07	3.0 – 3.2
7	20	1.9 ± 0.05	1.9 – 2.0
8	23.3	1.2 ± 0.03	1.2 – 1.3
9	26.7	1.0 ± 0.03	1.0 – 1.1

At dry conditions (0%), resistivity was very high at 1,867.4 Ω·m, reflecting the lack of conductive pore fluid. The addition of 3.3% seawater reduced resistivity drastically to 78.6 Ω·m, and further increases to 6.7% and 10% lowered resistivity to 25.9 Ω·m and 9.2 Ω·m, respectively. At higher moisture contents (>13.3%), resistivity stabilized at low values, between 6.0 and 1.0 Ω·m. This suggests that once a critical salinity threshold is reached, resistivity approaches an optimum conductive state, with additional seawater producing only minor changes.

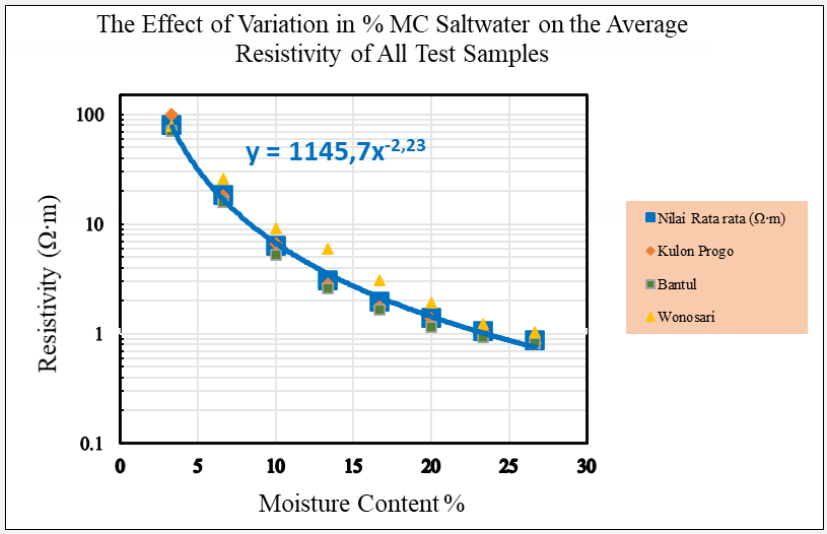

Figure 6. Effect of seawater moisture content (%) on the average resistivity of sand samples from all study sites (Kulonprogo, Bantul, and Wonosari).

After site-specific results were obtained, the datasets were combined to generate an average relationship across the three sites. This averaging was intended to provide a general representation of seawater influence on resistivity in coastal sand deposits. Figure 6 shows that resistivity decreases systematically with seawater content, spanning the range of 0.8–99.3 Ω·m. The relationship follows a power law:

$$R = 1145.7MC^{-2.23} \quad (11)$$

where R is resistivity and MC is seawater moisture content (%).

Table 4. Relationship between seawater content and average resistivity of unconsolidated sand samples from Kulonprogo, Bantul, and Wonosari

No	Seawater MC (%)	Resistivity (Ω·m)	Accuracy Range (Ω·m)
1	0	2062.6 ± 118.0	1944.6 – 2180.6
2	3.3	99.3 ± 1.82	97.5 – 101.1
3	6.7	18.2 ± 0.34	17.9 – 18.5
4	10	6.7 ± 0.13	6.5 – 6.8
5	13.3	2.8 ± 0.06	2.8 – 2.9
6	16.7	1.8 ± 0.04	1.7 – 1.8
7	20	1.4 ± 0.04	1.3 – 1.4
8	23.3	1.0 ± 0.03	1.0 – 1.1
9	26.7	0.8 ± 0.03	0.8 – 0.8

Dry samples averaged 2,062.6 Ω·m, confirming the highly resistive nature of unconsolidated sand. At only 3.3% seawater content, resistivity dropped drastically to 99.3 Ω·m, with a continued decline to 6.7 Ω·m at 10%. Beyond 13.3%, resistivity values stabilized between 2.8 and 0.8 Ω·m, which may be taken as a cutoff threshold indicating seawater intrusion conditions.

Comparison with previous field studies demonstrates consistency. For example, seawater intrusion was identified at 0.5–30 Ω·m in Candidasa (Pujianiki & Simpen, 2018), 2.07–13.2 Ω·m in Kaligawe (Hastuti et al., 2015), 4.95–31.9 Ω·m in Karimunjawa (Pryambodo & Prihantono, 2017), and 0.15–28.10 Ω·m in Mempawah (Muhardi et al., 2020). Collectively, these results indicate that seawater intrusion in coastal aquifers is generally associated with resistivity values between <1 and 30 Ω·m.

The power-law function $R = 1145.7MC^{-2.23}$ derived from the experimental dataset provides a quantitative framework for interpreting seawater saturation in sandy coastal aquifers. This empirical relationship strengthens the application of geoelectrical resistivity methods for detecting and delineating seawater intrusion. Furthermore, the contrast between dry and seawater-treated samples underscores the importance of ion content in controlling subsurface resistivity and supports the use of resistivity cutoffs in coastal groundwater monitoring, particularly for the Yogyakarta coastal aquifers.

CONCLUSION

Based on the results and discussion, the following key conclusions can be drawn:

1. Resistivity decreases exponentially with increasing seawater content and tends to stabilize at moisture contents above 13%. At this stage, resistivity values range between 0.8 and 2.8 Ω·m, which may serve as a cutoff threshold for identifying seawater intrusion.
2. The resistivity of dry sand samples without seawater content (0% MC) ranged between 1,944.6 and 2,180.6 Ω·m.
3. Experimental results from the Yogyakarta coast show that the relationship between resistivity (R) and seawater moisture content (MC) is described by the power-law function $R = 1145.7MC^{-2.23}$, which can be applied to improve the precision of geoelectrical interpretations.

Limitations

This study has several limitations. First, it did not examine the effect of varying proportions of freshwater and seawater on resistivity. Second, the laboratory experiments were limited to homogeneous sand samples and did not account for the heterogeneity of grain textures. Finally, the influence of mineral composition on resistivity was not evaluated, even though variations in mineral conductivity could also significantly affect resistivity measurements.

Acknowledgments

The authors would like to express their gratitude to the Geophysics Engineering Laboratory and the Institute for Research and Community Service (LPPM), UPN "Veteran" Yogyakarta, for providing financial support, facilities, and technical assistance throughout the implementation of this research.

REFERENCES

Afriyanto, A., Nugraha, A. L., & Firdaus, H. S. (2020). Analisis kesesuaian kawasan wisata pantai di Kabupaten Gunungkidul, Daerah Istimewa Yogyakarta. *Jurnal Geodesi Undip, 9*(3), 22–30. https://doi.org/10.14710/jgundip.2020.28106

Águila, J. F., Rowan, T. S. L., McDonnell, M. C., Etsias, G., & Chambers, J. E. (2025). Time-lapse resistivity imaging and self-potential monitoring of experimentally induced saline intrusion in coastal aquifer sands. Science of the Total Environment, 867, 161442. https://doi.org/10.1016/j.scitotenv.2023.161442

Ardaneswari, T. A., Yulianto, T., & Putranto, T. T. (2016). Analisis intrusi air laut menggunakan data resistivitas dan geokimia air tanah di dataran aluvial Kota Semarang. *Youngster Physics Journal, 5*(4), 335–350. https://ejournal3.undip.ac.id/index.php/bfd/article/view/14116

Arliska, E. A., Anda, P., & Hasan, E. S. (2022). Identifikasi intrusi air laut menggunakan metode vertical electrical sounding di Kecamatan Sawa. *Jurnal Geofisika Eksplorasi, 8*(3), 197–209. https://doi.org/10.23960/jge.v8i3.223

ASTM International. (2019). ASTM D2216-19: Standard Test Method for Laboratory Determination of Water (Moisture) Content of Soil and Rock by Mass. ASTM International. https://www.astm.org/d2216-19.html

ASTM International. (2020). ASTM G57-20: Standard Test Method for Measurement of Soil Resistivity Using the Wenner Four-Electrode Method. ASTM International. https://www.astm.org/G0057-20

Astutik, P., Wahyono, S. C., & Siregar, S. S. (2016). Identifikasi intrusi air laut menggunakan metode geolistrik di Desa Kampung Baru, Tanah Bumbu. *Jurnal Fisika FLUX, 13*(2), 155–160. https://doi.org/10.20527/flux.v13i2.3529

Dobrin, M. B., & Savit, C. H. (1988). Introduction to Geophysical Prospecting (4th ed.). McGraw-Hill Book Company.

Fondriest Environmental, Inc. (2014). Turbidity, total suspended solids and water clarity: Fundamentals of environmental measurements. Fondriest Environmental. https://www.fondriest.com/environmental-measurements/parameters/water-quality/turbidity/

Funtowicz, S., & Ravetz, J. R. (1990). Uncertainty and Quality in Science for Policy. Kluwer Academic Publishers.

Goebel, M., Pidlisecky, A., & Knight, R. (2017). Resistivity imaging reveals complex pattern of saltwater intrusion along Monterey coast. Journal of Hydrology, 551, 746–755. https://doi.org/10.1016/j.jhydrol.2017.02.037

Hasrianto, A., Imran, A., & Afasedanya, M. M. T. (2023). Identifikasi sebaran intrusi air laut berdasarkan peta ISO resistivitas metode geolistrik Kota Makassar. *Jurnal Teknik AMATA, 4*(1), 52–57. https://doi.org/10.55334/jtam.v4i1.109

Hastuti, D., Ramdhani, F., Waskito, F., Virgiawan, G., Febrika, G. Y., & Setyawan, A. (2015). Aplikasi metode geolistrik untuk menyelidiki intrusi air laut di kawasan pantai Kota Semarang (Kaligawe). *Youngster Physics Journal, 4*(4), 317–322. https://doi.org/10.14710/bfd.v4i4.9411

Hermans, T., & Paepen, M. (2020). Combined inversion of land and marine electrical resistivity tomography for submarine groundwater discharge and saltwater intrusion characterization. Geophysical Research Letters, 47(18), e2019GL085877. https://doi.org/10.1029/2019GL085877

Ikhsan, C., Haraty, S. R., & Juarzan, L. O. I. (2024). Identifikasi intrusi air laut pada air tanah menggunakan metode geolistrik tahanan jenis Wenner-Schlumberger (2D) di Pulau Balu, Desa Santiri, Kecamatan Tiworo Utara, Kabupaten Muna Barat. *Jurnal Rekayasa Geofisika Indonesia, 6*(1), 16–28.

Jusmi, F., & Bakri, K. (2020). Identifikasi kedalaman air tanah dan intrusi air laut dengan metode geolistrik konfigurasi Schlumberger di Desa Benteng, Kecamatan Malangke. *Jurnal Pendidikan Fisika, 14*(2), 38–44. https://doi.org/10.20527/jpf.v14i2.6974

Laiskodat, D. E., & Lay, B. P. (2023). Pengaruh pembangunan di pemukiman pesisir pantai di Kelurahan Oesapa terhadap rencana tata ruang Kota Kupang. *Jurnal Ilmiah dan Karya Mahasiswa, 1*(4), 369–382. https://doi.org/10.54066/jikma.v1i4.519

Mansourian, D., Smith, J., & Van den Berg, T. (2023). Geophysical surveys for saltwater intrusion assessment using electrical resistivity tomography and electromagnetic induction methods. Journal of Environmental and Soil Physics, 37(2), 145–160. https://doi.org/10.22059/JESPHYS.2022.324755.1007328

McDonnell, M. C., Flynn, R., Águila, J. F., Hamill, G. A., Donohue, S., Benner, E. M., Thomson, C., Etsias, G., Rowan, T. S. L., Wilkinson, P. B., Meldrum, P. I., & Chambers, J. E. (2023). Four-dimensional electrical resistivity imaging for monitoring pumping-induced saltwater intrusion in a coastal aquifer. Science of the Total Environment, 867, 161442. https://doi.org/10.1016/j.scitotenv.2023.161442

Mela, M. (2023). Pemetaan intrusi air laut terhadap air tanah di Pantai Gandoriah menggunakan metode geolistrik. *Jurnal Fisika Universitas Andalas, 13*(1), 45–50. https://doi.org/10.25077/jfu.13.1.45-50.2023

Muhardi, M., Faurizal, & Widodo. (2020). Analisis pengaruh intrusi air laut terhadap keberadaan air tanah di Desa Nusapati, Kabupaten Mempawah menggunakan metode geolistrik resistivitas. *Indonesian Journal of Applied Physics, 10*(2), 89–96. https://doi.org/10.22146/ijap.38125

Muslim, M., Azwar, A., & Muhardi, M. (2021). Identifikasi sebaran intrusi air laut di sekitar area Pelabuhan Internasional Kijing, Kabupaten Mempawah menggunakan metode resistivitas. *Jurnal Fisika, 11*(1), 19–26. https://doi.org/10.15294

Nisa, K., Yulianto, T., & Widada, S. (2012). Aplikasi metode geolistrik tahanan jenis untuk menentukan zona intrusi air laut di Kecamatan Genuk Semarang. *Berkala Fisika, 15*(1), 7–14. https://ejournal.undip.ac.id/index.php/berkala_fisika/article/view/4977

Nugroho, D., Subagio, H., Rachmadi, H., Kadesti, A. T., & Kintawangi, L. G. (2023). Tata ruang pesisir Bantul dalam perspektif keistimewaan Daerah Istimewa Yogyakarta. *GLOBAL: Jurnal Lentera BITEP, 1*(2), 76–89. https://doi.org/10.59422/global.v1i02.147

Pryambodo, D. G., & Prihantono, J. (2017). Pendugaan sebaran air payau dengan tomografi geolistrik di Pulau Karimunjawa, Jawa Tengah. *Jurnal Kelautan Nasional, 12*(1), 27–32. https://doi.org/10.15578/jkn.v12i1

Pujianiki, N. N., & Simpen, I. N. (2018). Aplikasi geolistrik pada pemetaan daerah intrusi air laut di Pantai Candidasa. *Media Komunikasi Teknik Sipil, 24*(1), 29–34. https://doi.org/10.14710/mkts.v24i1.17574

Putra, I. N. D, Suarbawa, K. N., & Wibawa, I. M. S. (2013). Pendeteksian intrusi air laut dengan metode geolistrik resistivitas konfigurasi Wenner di Desa Candikusuma, Kabupaten Jembrana, Bali. *Buletin Fisika, 14*(1), 12–17. https://doi.org/10.24843/BF.2013.v14.i01.p02

Putri, Y. D., Pujiastuti, D., & Afdal, A. (2020). Penentuan zona intrusi air laut di area Pelabuhan Perikanan Samudera Bungus menggunakan metode geolistrik tahanan jenis konfigurasi Wenner dua dimensi. *Jurnal Fisika Unand, 9*(4), 465–471. https://doi.org/10.25077/jfu.9.4

Sastrawan, F. D., Rahmania, R., & Arisalwadi, M. (2021). Studi awal indikasi intrusi air laut menggunakan metode geolistrik tahanan jenis. *Jurnal Fisika Flux, 18*(2), 164–169. https://doi.org/10.20527/flux.v18i2.9077

Smith, B. L., & Neal, D. R. (2022). Measurement Uncertainty. Utah State University.

Suritohardoyo, S. (2016). Perubahan permukiman perdesaan pesisir Kabupaten Gunung Kidul Daerah Istimewa Yogyakarta tahun 1996–2003. *Forum Geografi, 21*(1), 1–17. https://doi.org/10.23917/forgeo.v21i1.1817

Telford, W.M., Geldart, L.P., & Sheriff, R.E. (1990). Applied Geophysics (Edisi ke-2). Cambridge University Press. ISBN: 978-0521339384.

Trung, N. N., Phong, Đ. X., Thu, T. H., Nam, B. V., & Điệp, N. V. (2025). Mapping freshwater and seawater intrusion using electrical resistivity tomography and physicochemical data: An application in Coto Island, Gulf of Tonkin. Marine Geophysical Research, 46(1), 1–7. https://doi.org/10.1007/s11001-025-09562-x